HYAL1 Hyaluronidase in Prostate Cancer: A Tumor Promoter and Suppressor

Vinata B. Lokeshwar,[1,2,4] Wolfgang H. Cerwinka,[1] Tadahiro Isoyama,[1] and Bal L. Lokeshwar[1,3,4]

Departments of [1]Urology, [2]Cell Biology and Anatomy, and [3]Radiation Oncology, and [4]Sylvester Comprehensive Cancer Center, Miller School of Medicine, University of Miami, Miami, Florida

Abstract

Hyaluronidases degrade hyaluronic acid, which promotes metastasis. HYAL1 type hyaluronidase is an independent prognostic indicator of prostate cancer progression and a biomarker for bladder cancer. However, it is controversial whether hyaluronidase (e.g., HYAL1) functions as a tumor promoter or as a suppressor. We stably transfected prostate cancer cells, DU145 and PC-3 ML, with HYAL1-sense (HYAL1-S), HYAL1-antisense (HYAL1-AS), or vector DNA. HYAL1-AS transfectants were not generated for PC-3 ML because it expresses little HYAL1. HYAL1-S transfectants produced ≤42 milliunits (moderate overproducers) or ≥80 milliunits hyaluronidase activity (high producers). HYAL1-AS transfectants produced <10% hyaluronidase activity when compared with vector transfectants (18-24 milliunits). Both blocking HYAL1 expression and high HYAL1 production resulted in a 4- to 5-fold decrease in prostate cancer cell proliferation. HYAL1-AS transfectants had a G_2-M block due to decreased cyclin B1, cdc25c, and cdc2/p34 expression and cdc2/p34 kinase activity. High HYAL1 producers had a 3-fold increase in apoptotic activity and mitochondrial depolarization when compared with vector transfectants and expressed activated proapoptotic protein WOX1. Blocking HYAL1 expression inhibited tumor growth by 4- to 7-fold, whereas high HYAL1 producing transfectants either did not form tumors (DU145) or grew 3.5-fold slower (PC-3 ML). Whereas vector and moderate HYAL1 producers generated muscle and blood vessel infiltrating tumors, HYAL1-AS tumors were benign and contained smaller capillaries. Specimens of high HYAL1 producers were 99% free of tumor cells. This study shows that, depending on the concentration, HYAL1 functions as a tumor promoter and as a suppressor and provides a basis for anti-hyaluronidase and high-hyaluronidase treatments for cancer. (Cancer Res 2005; 65(17): 7782-9)

Introduction

Hyaluronidase is an endoglycosidase that degrades hyaluronic acid. Hyaluronic acid is a glycosaminoglycan made up of repeating disaccharide units D-glucuronic acid and *N*-acetyl-D-glucosamine (1, 2). In addition to maintaining hydration status and osmotic balance in tissues, hyaluronic acid interacts with cell surface receptors, such as CD44 and receptor for hyaluronic acid–mediated motility, and regulates cell adhesion, migration, and proliferation (1–3). Hyaluronic acid concentration is elevated in several tumors, including carcinomas of breast, colon, prostate, and bladder (4–8). We have shown that increased urinary hyaluronic acid levels serve as an accurate marker for detecting bladder cancer, regardless of the tumor grade (9, 10). In prostate cancer tissues, hyaluronic acid is mainly produced by tumor-associated stroma; however, ~40% of tumor cells express hyaluronic acid (11, 12). Tumor-associated hyaluronic acid promotes tumor cell migration, aids in the loss of contact inhibition, and offers protection against immune surveillance (13–15). Small hyaluronic acid fragments (3-25 disaccharide units), generated by hyaluronidase, are angiogenic (16, 17). We have detected such fragments in prostate cancer tissues, in bladder cancer patients' urine, and in the saliva of head and neck cancer patients (7, 9, 18).

Hyaluronidase is crucial for the spread of bacterial infections, toxins, and venoms (19, 20). The human genome contains six hyaluronidase genes, found on two chromosomes: 3p 21.3 (HYAL1, HYAL2, and HYAL3) and 7q 21.3 (HYAL4, PH20, and HYALP1; ref. 21). PH20 or testicular hyaluronidase induces the acrosomal reaction during ovum fertilization (22). HYAL1 is present in human serum and urine and has a pH optimum of ~4.2. HYAL1 is 50% active at pH 4.5 (7, 23, 24). Lack of functional HYAL1 causes a mild disorder called type IX mucopolysaccharidosis (25). It is also the major hyaluronidase expressed in cancers of the prostate, bladder, and head and neck, and is secreted by tumor cells (7, 11, 18, 26). In bladder cancer, increased hyaluronidase levels (i.e., HYAL1) serve as an accurate marker for detecting high-grade tumors (6, 9, 10). Using radical prostatectomy specimens from patients with a 6- to 10-year follow-up, we found that HYAL1 is an independent predictor of biochemical recurrence (i.e., disease progression; refs. 11, 12). Hyaluronidase levels also increase in breast cancer cells when they become metastatic (27, 28). We recently showed that blocking HYAL1 expression in an invasive bladder cancer line decreases tumor growth by 9- to 17-fold, inhibits tumor infiltration, and decreases microvessel density 4- to 9-fold (29). Expression of HYAL1 in PC-3 prostate cancer cells that produce low levels of hyaluronidase causes a slight increase in lung metastasis (30). These observations show that hyaluronidases in general, and HYAL1 in particular, are tumor promoters.

Contrary to the tumor growth– and metastasis-promoting effects of HYAL1, the chromosomal locus (i.e., 3p 21.3) that encodes the *HYAL-1*, *HYAL-2*, and *HYAL-3* genes is deleted in some epithelial tumors at high frequency, although the tumor suppressor gene in this locus is not one of the hyaluronidase genes (31–33). HYAL2 levels are also slightly decreased in high-grade B-cell non-Hodgkin's lymphomas (34). Overexpression of HYAL1 in a rat colon carcinoma line inhibits tumor growth and generates necrotic tumors (35). Administration of super high concentrations of bovine testicular hyaluronidase (300 units) causes a 50% regression of breast tumor xenografts (36).

Note: T. Isoyama is currently at Tottori University Hospital, Yonago, Japan.
Requests for reprints: Vinata B. Lokeshwar, Department of Urology (M-800), Miller School of Medicine, University of Miami, P.O. Box 016960, Miami, FL 33101. Phone: 305-243-6321; Fax: 305-243-6893; E-mail: vlokeshw@med.miami.edu.

doi:10.1158/0008-5472.CAN-05-1022

Furthermore, transient expression of HYAL1 and HYAL2 in L929 mouse fibroblasts or treatment of these cells with super high concentrations of bovine testicular hyaluronidase (100 units/mL) increases tumor necrosis factor–mediated cytotoxicity by inducing the expression of a proapoptotic protein WOX1 (a ww domain–containing oxidoreductase; refs. 37–40). In these cells, WOX1 induces apoptosis following its activation by phosphorylation on Tyr-33 residue (WOX1-^{P}Tyr-33) and its translocation to mitochondria and then into the nucleus (38). These observations suggest that hyaluronidases, including HYAL1, are tumor suppressors.

At present, no studies have been conducted to explain the contradictory findings about HYAL1 function in tumor growth and invasion. To discern the tumor-promoting and tumor-suppressing functions of HYAL1, we stably transfected androgen-independent prostate cancer cell lines DU145 and PC-3 ML to generate moderate HYAL1 producers, high HYAL1 producers, and no/little HYAL1 producers. Our results show that HYAL1 is both a tumor promoter and a suppressor, depending on its concentration.

Materials and Methods

Generation of HYAL1-S and HYAL1-AS stable transfectants. The HYAL1 coding region was cloned into a eukaryotic expression vector, pcDNA3.1/v5-His TOPO, in the sense (HYAL1-S) and antisense (HYAL1-AS) orientation, with respect to the cytomegalovirus promoter (29). DU145 and PC-3 ML cells (1×10^5/6-cm dish) were transfected with vector, HYAL1-S, or HYAL1-AS cDNA constructs (1 μg DNA) using Effectene (Qiagen). Transfectant clones were selected in a growth medium (RPMI 1640 + 10% fetal bovine serum + gentamicin) plus geneticin (Invitrogen, Carlsbad, CA).

Analysis of hyaluronidase activity and HYAL1. Hyaluronidase activity secreted by transfectants into serum-free conditioned media was measured using a hyaluronidase ELISA-like assay and expressed as milliunits per 10^6 cells (41). Both the active hyaluronidase species and HYAL1 were identified in the transfectant conditioned media (secreted by 5×10^4 cells, ~10 μg total protein) with substrate (hyaluronic acid)-gel electrophoresis and immunoblot analysis, using a rabbit anti-HYAL1 immunoglobulin G (IgG), respectively (26).

Immunoblot analysis and kinase assay. Cell lysates (4×10^4 cells) were immunoblotted using anti-cyclin B1 IgG, anti-cdc2/p34 IgG, anti-cdc25c IgG, or anti-actin IgG (Lab Vision Corp./Neomarkers, Fremont, CA; ref. 29). cdc2/p34 kinase was immunoprecipitated from cell lysates (1×10^6 cells/transfectant) using an anti-cdc2/p34 antibody. Immunoprecipitates were used for the cdc2/p34-associated H1 histone kinase activity assay using H1 histone (29). Cell lysates were also immunoblotted using rabbit anti-WOX1 and rabbit anti-WOX1 phosphospecific Tyr-33 IgG (1:3,000 dilution; EMD Biosciences, San Diego, CA).

Cell proliferation assay. Transfectant clones were cultured on 24-well plates in growth medium + geneticin. Cells were counted in duplicate wells every 24 hours, for a total period of 120 hours, in two independent experiments.

Cell cycle analysis. Cell cycle phase distribution in actively growing transfectant cultures was estimated by propidium iodide staining of DNA and flow cytometry using an EPICS XL flow cytometer (29). FL3 histograms were analyzed using the Modfit Easy (Lite) Program (Veritas Software ME). Samples were assayed in duplicate in two independent experiments.

Apoptosis assays. Ninety-six-hour cultures of transfectants (10^5 cells/24-well plate) were lysed and the cell lysates were tested for free nucleosome release using the Cell Death ELISA kit (Roche Diagnostics, Pleasanton, CA). Annexin V binding was examined in 96-hour cultures of transfectants (~3×10^5 cells/6-cm dish) using the ApoAlert Annexin V-enhanced green fluorescent protein kit (BD Clontech Labs, Mountain View, CA) and flow cytometry. Median fluorescence intensity (Annexin V binding to phosphatidylserine) was compared among the transfectants in the green fluorescence channel (log FL1). Mitochondrial depolarization was examined by incubating actively growing cultures of transfectants with a mitochondria-specific dye, JC-1, for 15 minutes followed by flow cytometry. An increase in the green fluorescence intensity was approximated as a decrease in mitochondrial membrane potential ($\Delta\Psi$; ref. 42).

Matrigel invasion assay. Transfectants (3×10^5 cells) were plated on the upper chamber of a Matrigel-coated transwell plate in serum-free medium. The bottom chamber contained growth medium. After 48 hours, invasion of cells through the Matrigel into the bottom chamber was quantified using the 3-(4,5-dimethylthiazol-2-yl)-2,5-diphenyltetrazolium bromide assay. Cell invasion was calculated as (cells in the bottom chamber ÷ cells in upper + bottom chambers) × 100 (29).

Pericellular matrix assay. Formaldehyde-fixed human erythrocytes were overlaid on transfectants, which were cultured for 24 hours (10^4 cells/6-cm dish). Cells showing a bright region around the entire periphery with width equal to or greater than the diameter of an erythrocyte (i.e., pericellular matrix) were counted in 10 fields. Results were expressed as percentage of cells with pericellular matrix ± SD (29, 43).

Tumor xenografts and histology. Transfectants (2×10^6 cells) were s.c. implanted on the dorsal flank of 5-week-old male athymic mice (10/clone). After the tumors became palpable, the tumor size was measured twice weekly. Tumor volume was approximated to an ellipsoid (44). Following euthanasia (DU145: 42 day; PC-3 ML: 28 day), the tumors were weighed. Tukey's multiple comparison test was used to evaluate the differences in tumor growth rate and tumor weight. Tumor histology was done at Charles River Laboratories (Wilmington, MA).

Hyaluronic acid, HYAL1 localization, and microvessel density determination. Hyaluronic acid and HYAL1 were localized in tumor xenograft specimens by immunohistochemistry using a biotinylated hyaluronic acid–binding protein and the anti-HYAL1 IgG, respectively (29). Microvessel density was evaluated using CD34 staining (rat anti-mouse CD34 IgG; BD PharMingen, Mountain View, CA; ref. 29). Microvessel density was determined by two readers independently counting microvessels in 10 fields and expressed as mean ± SD. The length of the microvessels was measured using a Nikon H550L microscope with a video screen camera equipped with measuring tools.

Results

Analysis of HYAL1 expression in DU145 and PC-3 ML transfectants. Whereas DU145 cells secrete hyaluronidase activity into their conditioned media, PC-3 ML cells secrete very little hyaluronidase (7). We generated HYAL1-S (hyaluronidase overproducing) transfectants of both DU145 and PC-3 ML cells, but only HYAL1-AS transfectants of DU145. We analyzed 25 to 30 clones of each transfectant type for hyaluronidase production and HYAL1 expression. We selected two types of HYAL-S transfectants, moderate hyaluronidase overproducing and high hyaluronidase overproducing. Data on two clones from each type are shown. As shown in Fig. 1*A-a*, when compared with vector #1 and #2 clones, DU145 HYAL1-S clones #1 and #2 secrete 1.5- to 2.3-fold more hyaluronidase activity (moderate overproducers). HYAL1-S #3 and #4 clones (high producers) secrete 3.8- to 7.3-fold more hyaluronidase activity than the vector clones (Fig. 1*A-a*). There is >90% reduction in hyaluronidase secretion in HYAL1-AS clones. PC-3 ML HYAL1-S clones #1 and #2 secrete 10-fold more hyaluronidase activity than that secreted by PC-3 ML vector clones (Fig. 1*A-b*). HYAL1-S #3 and #4 clones secrete 80 to 100 milliunits hyaluronidase activity, which is similar to that secreted by DU145 #3 and #4 clones.

Anti-HYAL1 immunoblot analysis shows that a ~60 kDa HYAL1 protein is secreted in the conditioned media of DU145 vector and HYAL1-S clones but not in HYAL1-AS clones (Fig. 1*B-a*). In PC-3 ML clones, HYAL1 protein is detected in the conditioned media of HYAL1-S transfectants but not in vector clones. The amount of

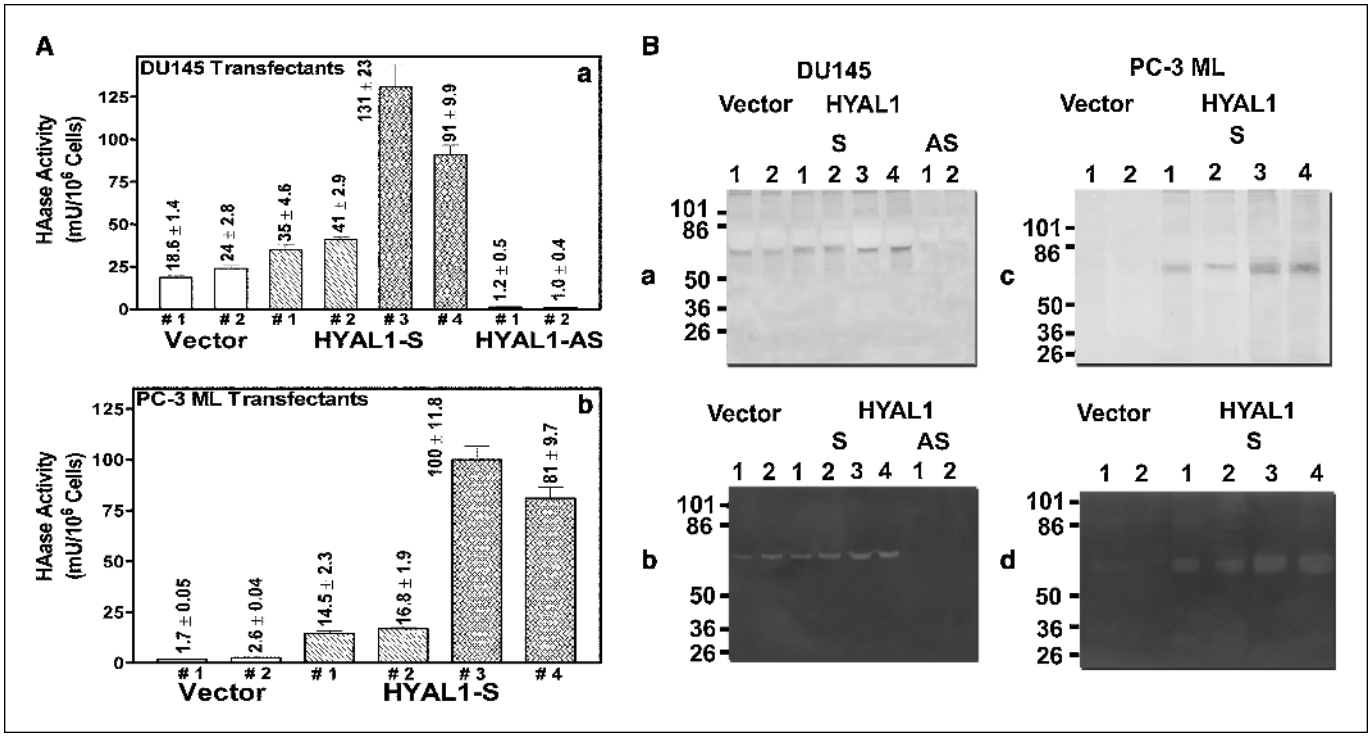

Figure 1. Analysis of hyaluronidase activity in DU145 and PC-3 ML transfectants. *A,* hyaluronidase activity (milliunits per milligram) was measured using an ELISA-like assay. *Columns,* mean (triplicates in three experiments); *bars,* SD. *B,* detection of HYAL1 expression by immunoblot and substrate (hyaluronic acid)-gel assay. *A* and *C,* immunoblot analysis. Conditioned media (10 μg protein; conditioned media of 50,000 cells) were subjected to anti-HYAL1 IgG immunoblotting. *B* and *D,* substrate (hyaluronic acid)-gel assay. Conditioned media (10 μg protein; conditioned media of 50,000 cells) were analyzed by substrate (hyaluronic acid)-gel electrophoresis.

HYAL1 protein detected in HYAL1-S clones #3 and #4 is higher than that detected in HYAL1-S #1 and #2 clones (Fig. 1*B-b*). The substrate (hyaluronic acid)-gel analysis confirms immunoblot results and detects a ~60 kDa active hyaluronidase species in the conditioned media of DU145 vector and HYAL1-S clones and in PC-3 ML HYAL1-S clones (Fig. 1*B-c* and *B-d*).

Effect of HYAL1 expression on cell proliferation and cell cycle. The growth rates of DU145 vector and HYAL1-S #1 and #2 transfectants are comparable (doubling time, ~26-28 hours; Fig. 2*A*). However, both HYAL1-AS clones and HYAL1-S #3 and #4 clones (which secrete ≥100 milliunits/10^6 hyaluronidase activity) grow 4- to 5-fold slower than vector clones (doubling time, ~90-96 hours). PC-3 ML HYAL1-S #1 and HYAL1-S #2 clones grow 1.5- to 2-fold faster than the vector clones; however, the high HYAL1 producing clones, HYAL1-S #3 and #4, grow 2- to 2.5-fold slower than the vector clones (Fig. 2*B*).

Cell cycle analysis showed that the decreased growth rate of HYAL1-AS transfectants was due to cell cycle arrest in the G_2-M phase. There was a 200% to 300% increase in the number of HYAL1-AS #1 and #2 cells in G_2-M phase (22.3% and 31.3%, respectively) when compared with vector (#1: 11.5%, #2: 12.4%) and all HYAL1-S transfectant (9.7-12.1%) clones. This increase in the G_2-M phase was statistically significant ($P < 0.001$, Tukey's test). Correspondingly, the percentage of HYAL1-AS cells in S phase was lower (#1: 28.8%, #2: 24.8%) when compared with vector (#1: 35.9%; #2: 37.2%) and HYAL1-S (#1: 36.4%; #2: 38.5%) cells. There was no change in the percentage of cells in G_0-G_1 phase in any of the transfectants. In PC-3 ML transfectants, HYAL1 expression also increased the number of cells in the S phase with a corresponding decrease in the number of cells in G_2-M phase (data not shown).

The expression of G_2-M regulators (i.e., cdc25c, cyclin B1, and cdc2/p34 proteins) was analyzed in various clones by immunoblotting. As shown in Fig. 2*C*, both cdc25c bands, plausibly representing phosphorylated (slow-moving) and native forms, are detected in all DU145 transfectants. There is an ~3-fold decrease in the expression cdc25c and cyclin B1, as well as a 2-fold decrease in cdc2/p34 expression in HYAL1-AS transfectants, when compared with the vector and HYAL1-S transfectant clones (Fig. 2*C*). A 2.5- and 3-fold decrease in cdc2/p34-associated H1 histone kinase activity is observed in HYAL1-AS transfectant clones when compared with vector and all HYAL1-S transfectants (Fig. 2*C*). These results show that the slow proliferation rate of HYAL1-AS transfectants is due to G_2-M arrest.

Effect of HYAL1 expression on apoptosis. Next we determined whether the slower growth of HYAL1-S #3 and #4 clones of DU145 and PC-3 ML cells was due to a high rate of apoptosis. As shown in Fig. 3*A*, there was a 3-fold increase in the intracellular levels of free nucleosomes (i.e., increased apoptotic activity) in DU145 HYAL1-S #3 and HYAL1-S #4 clones when compared with vector, HYAL1-S #1 and #2, as well as HYAL1-AS clones. Similar results were obtained for PC-3 ML transfectants.

To confirm the induction of apoptosis, we measured the outward translocation of plasma membrane phosphatidylserine by Annexin V binding. As shown in Fig. 3*B*, there is a distinct increase in enhanced green fluorescent protein-Annexin V binding to the surface of HYAL1-S #3 and #4 cells when compared with vector control (i.e., right shift in log FL1; median peak log FL1: vector, 1.21; HYAL1-S #3, 2.37; HYAL1-S #4, 2.83).

We next examined mitochondrial involvement in high-HYAL1–mediated increase in apoptosis using the JC-1 dye binding assay

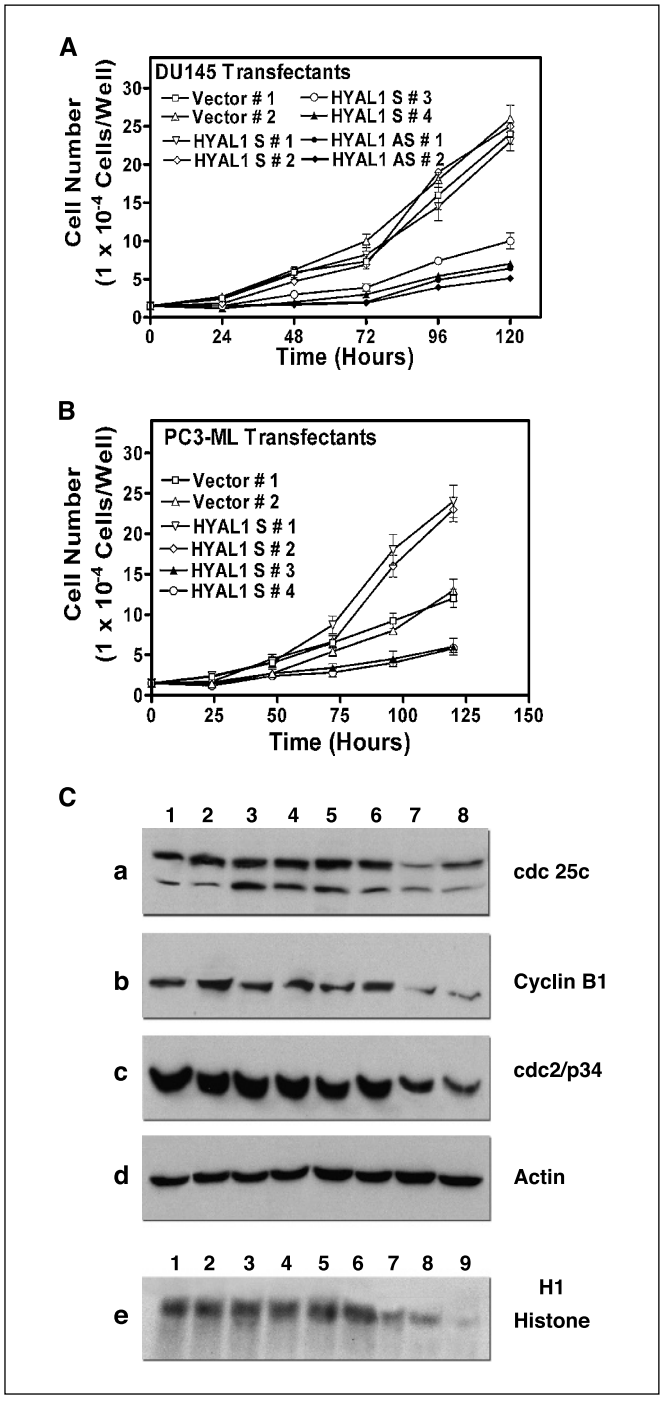

Figure 2. *A* and *B,* determination of proliferation rate of transfectants. *Points,* mean from duplicate measurements (three independent experiments); *bars,* SD. *A,* DU145; *B,* PC-3 ML. *C,* analysis of G_2-M cell cycle regulators. Cell lysates of DU145 transfectants were analyzed by immunoblotting using anti-cdc25c (*a*), anti-cyclin B1 (*b*), anti-cdc2/p34 (*c*), and β-actin (*d*) antibodies. *Lanes 1* and *2,* vector clones #1 and #2; *lanes 3* to *6,* HYAL1-S clones #1 to #4; *lanes 7* and *8,* HYAL1-AS clones #1 and #2. *e,* measurement of H1 histone kinase-associated activity. *Lanes 1* to *8,* the same as described above; *lane 9,* negative control.

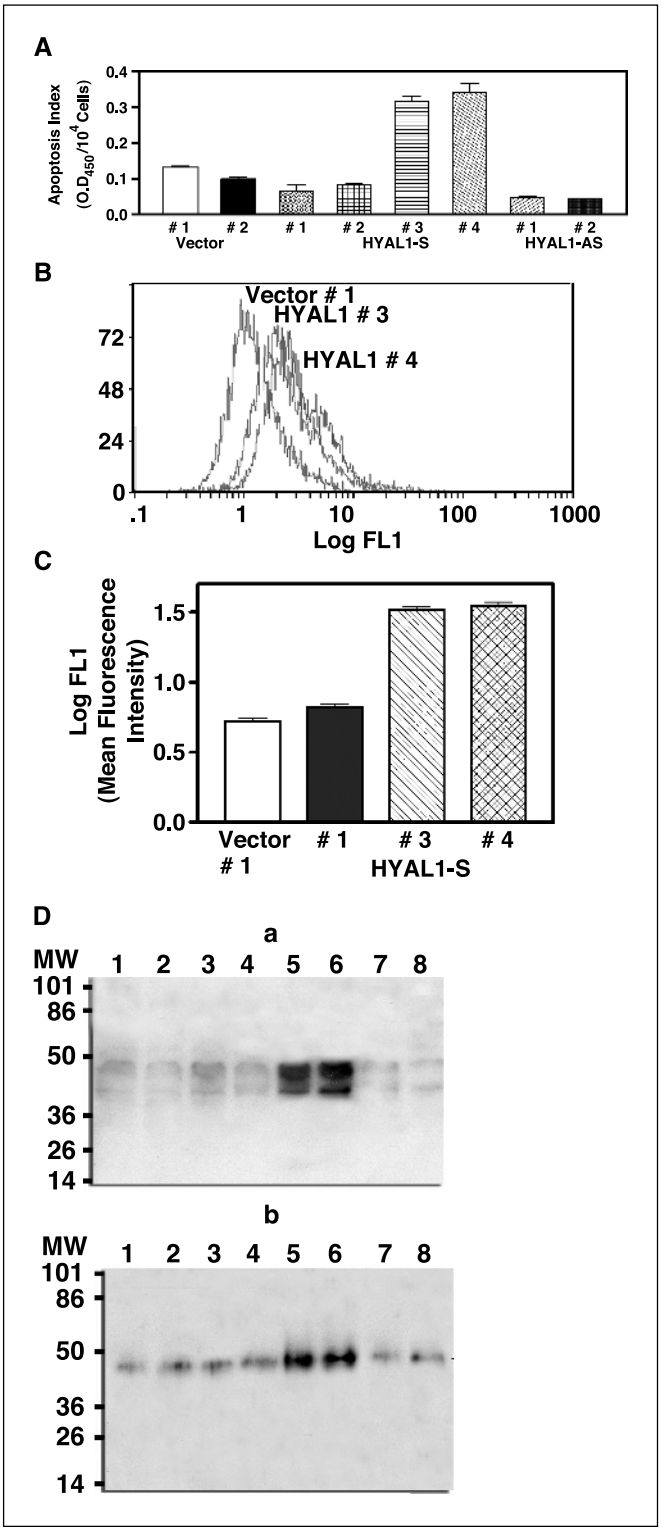

Figure 3. Examination of apoptosis. *A,* apoptotic activity in various transfectants was evaluated using the Cell Death ELISA Plus assay kit. *Columns,* mean (triplicates in two experiments); *bars,* SD. *B,* cell surface enhanced green fluorescent protein-Annexin V binding to translocated phosphatidylserine was analyzed in transfectants using flow cytometry. Experiment was repeated twice. *C,* mitochondrial depolarization was analyzed by JC-1 dye binding assay using flow cytometry. *Columns,* mean; *bars,* SD. *D,* cell lysates of DU145 transfectants were analyzed by immunoblotting using anti-WOX1 (*a*) and anti-WOX1 phosphospecific Tyr-33 antibodies (*b*). *Lanes 1* and *2,* vector clones #1 and #2; *lanes 3* to *6,* HYAL1-S clones #1 to #4; *lanes 7* and *8,* HYAL1-AS clones #1 and #2.

(42). As shown in Fig. 3*C*, HYAL1-S #3 and HYAL1-S #4 transfectants exhibit a 200% increase in log FL1, indicating a decrease in $\Delta\Psi$ (i.e., increased mitochondrial permeabilization) when compared with vector and moderate HYAL1 overexpressing clones.

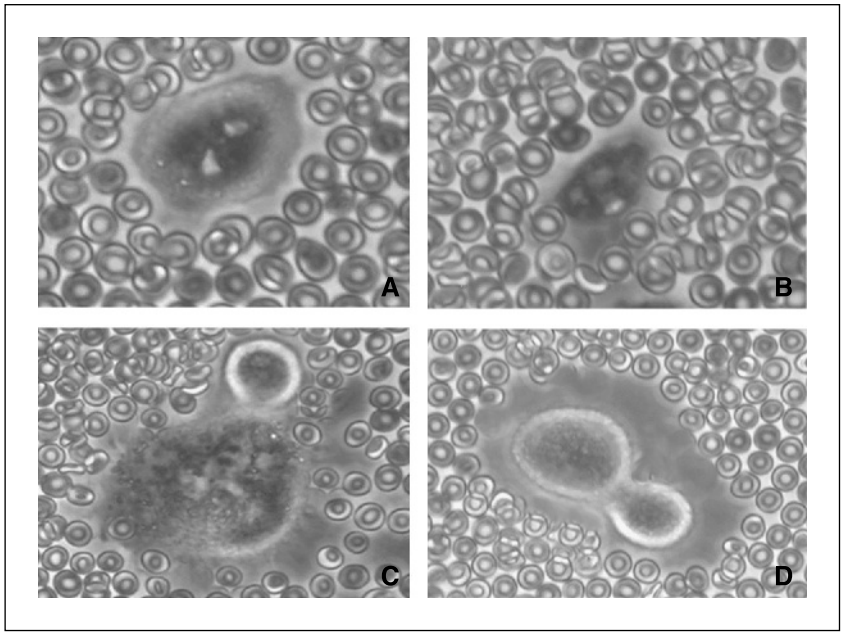

Figure 4. Examination of pericellular matrix in DU145 transfectants. Pericellular matrices surrounding DU145 transfectants were visualized using the particle exclusion assay. *A,* vector #1; *B,* HYAL1-S #1; *C,* HYAL1-S #4; *D,* HYAL1-AS #2.

We then examined the expression of the proapoptotic protein WOX1 and its activated form, WOX1-^{P}Tyr-33, in various transfectants. As shown in Fig. 3*D*, the major WOX1 isoform expressed in DU145 transfectants is 46 kDa WOX1-v1, although some expression of the 41 kDa WOX1-v2 isoform is also observed (Fig. 3*D-a*). The expression of both WOX1 isoforms is increased >3-fold in HYAL1-S #3 and #4 clones, when compared with vector, moderate HYAL1 expressing clones, and HYAL1-AS clones. The expression of the activated form of WOX1-v1 (WOX1-^{P}Tyr-33) is also increased >3-fold in HYAL1-S #3 and #4 clones. This suggests that increased apoptosis in high HYAL1 producing clones involves mitochondria and is possibly mediated by increased WOX1 expression and its activation.

Effect of HYAL1 expression on *in vitro* invasion. In the Matrigel invasion assay, the invasive activity of DU145 vector #1 clone (22.3 ± 4.3%) was normalized as 100%. The invasive activity of all HYAL1-S clones (#1-#4) varied between 109% and 118% and was not statistically different from that of vector clones ($P > 0.05$). However, the invasive activity of HYAL1-AS clones (28.2 ± 1.7% and 31.5 ± 1.5%) was 3-fold less when compared with vector clones ($P < 0.001$, Tukey's test). HYAL1 expression increased the invasive activity of PC-3 ML transfectants by 3- to 3.5-fold when compared with vector clones ($P < 0.001$). These results show that HYAL1 expression increases the invasive activity of prostate cancer cells.

Effect of HYAL1 expression on pericellular matrix formation. As shown in Fig. 4, vector #1 and HYAL1-S clones (#1 and #3) do not exhibit pericellular matrices as the erythrocytes closely abut the surface of each cell. However, HYAL1-AS cells (clone #1) exhibit a clear pericellular matrix. In 10 randomly selected fields (120-150 cells), the percentage of cells with pericellular matrix was 3- and 4.6-fold higher in the HYAL1-AS transfectants (#1: 94.2 ± 8.6%; #2: 86.3 ± 9.0%) when compared with vector (#1: 27.8 ± 18%; #2: 35.5 ± 11.1%), moderate HYAL1 overproducing (HYAL1-S #1: 25.5 ± 13.2%; #2: 31.2 ± 18%), and high HYAL1 overproducing (HYAL1-S #3: 22.3 ± 16.1%; #4: 17.2 ± 13.2%) transfectants, respectively ($P < 0.001$). Thus, hyaluronic acid is an important component of the pericellular matrix of prostate cancer cells and it is degraded by HYAL1.

Effect of HYAL1 expression on tumor xenografts. In xenografts, there is a 4- to 5-fold delay in the generation of palpable tumors in animals injected with DU145 HYAL1-AS transfectants (33 ± 4 days) when compared with vector and moderate HYAL1 overproducing transfectants (6-8 days; Fig. 5*A*, $P < 0.001$). Interestingly, high HYAL1 producers did not form palpable tumors even on day 40 when necropsy was done. Weights

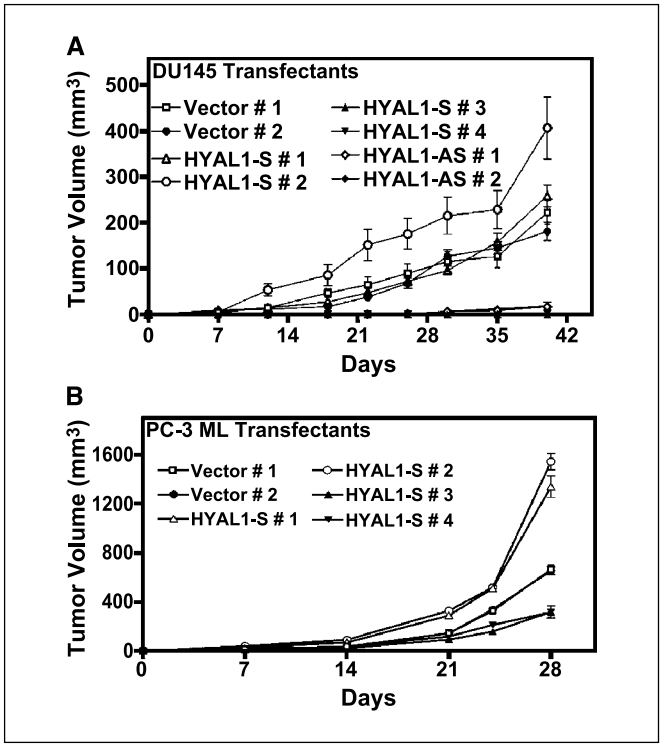

Figure 5. Examination of the growth of DU145 and PC-3 ML transfectant tumors in xenografts. DU145 and PC-3 ML transfectants were injected s.c. in athymic mice (10 animals/group) and tumor volume was measured as described in Materials and Methods. *Columns,* mean; *bars,* SD. *A,* DU145; *B,* PC-3 ML.

(in grams) of tumors generated by vector clones (#1: 0.17 ± 0.05; #2: 0.14 ± 0.04) and moderate HYAL1 overproducers (HYAL1-S #1: 0.21 ± 0.06; #2: 0.27 ± 0.14) were 4- to 7-fold higher than HYAL1-AS tumors (#1: 0.03 ± 0.01; #2: 0.04 ± 0.01), respectively ($P < 0.001$). HYAL1-S #1 and #2 tumors also showed the presence of large blood vessels. None of the animals injected with HYAL1-S #3 or #4 transfectants had visible evidence of tumor, although in some animals a Matrigel pluglike material was visible. Two additional high HYAL1 producing transfectants generated in a second transfection experiment also did not form palpable tumors (data not shown).

Moderate HYAL1 producing PC-3 ML tumors (HYAL1-S #1 and #2) grow about 2-fold faster, whereas high HYAL1 producing tumors grow 2- to 2.5-fold slower than vector tumors (Fig. 5*B*). At day 28, the weights (in grams) of moderate HYAL1 producing tumors (#1: 0.57 ± 0.12; #2: 0.6 ± 0.14) were ~2-fold higher than vector tumors (#1: 0.28 ± 0.06; #2: 0.29 ± 0.04) and 3.5-fold higher than high HYAL1 producing tumors (#3: 0.16 ± 0.03; #4: 0.14 ± 0.05; $P < 0.001$). Interestingly, PC-3 ML cells cultured from HYAL1-S #3 and #4 tumor tissues did not secrete any hyaluronidase activity and had lost HYAL1 expression. This suggests that *in vivo*, in the absence of a selecting agent (i.e., geneticin), HYAL1-S #3 and #4 transfectants reverted to wild-type, and therefore formed tumors (although the tumors were smaller than vector tumors).

Histology reports and photomicrographs show that DU145 vector and moderate HYAL1 producing tumors show high mitotic figures, invade skeletal muscle and lymph nodes, and infiltrate lymphatic and blood vessels. However, the tumors generated by HYAL1-AS transfectants are noninvasive (Fig. 6*A*). The Matrigel pluglike material removed from HYAL1-S #3 and #4 animals is ≥99% free of tumor cells and no mitotic figures are observed (Fig. 6*A*). Therefore, whereas blocking HYAL1 production significantly reduces tumor growth, its overproduction also decreases tumor growth and may even inhibit tumor incidence.

HYAL1, hyaluronic acid expression, and microvessel density in tumor xenografts. Tumor cells in vector and HYAL1-S #1 and #2 xenografts express significant levels of HYAL1, but HYAL1-AS cells do not secrete HYAL1 (Fig. 6*B*). Interestingly, as we observed in bladder cancer xenografts (29), hyaluronic acid production is increased in the tumor-associated stroma of vector and HYAL1-S #1 tumor specimens when compared with HYAL1-AS #1 tumor specimens (Fig. 6*B*). Microvessel density in vector (39.09 ± 4.6; #2: 36.5 ± 6.5) and moderate HYAL1 producing (HYAL1-S #1: 47.64 ± 13; #2: 51.3 ± 12.5) tumors is slightly higher than HYAL1-AS (#1: 34.3 ± 17.6; #2: 27.3 ± 12.1) tumors ($P > 0.05$). However, the length of the capillaries (in micrometers) in vector (817.4 ± 141.5) and HYAL1-S (#1: 1,031 ± 262.5; #2: 817.9 ± 305.3) tumors is 4- to 5-fold greater than the capillaries found in HYAL1-AS tumors (#1: 218.1 ± 103.4; #2: 247.1 ± 96.1; Fig. 6*C*).

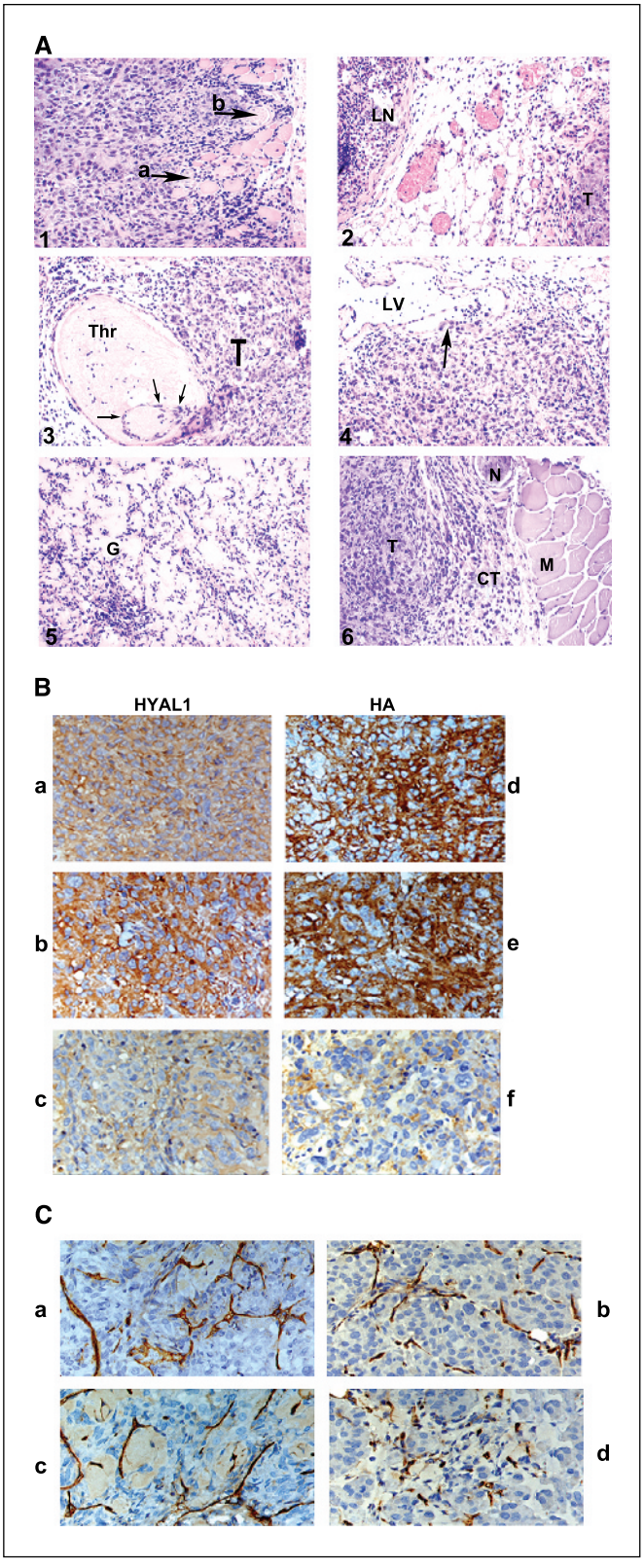

Figure 6. Examination of tumor histology. *A,* photomicrographs of H&E-stained tumor specimens are shown at ×100 magnification. *1,* vector #1: muscle fibers are surrounded by tumor cells (*arrow a*) and the tumor impinges on an adjacent nerve (*arrow b*). *2,* vector #2: tumor (*T*) approaches a lymph node (*LN*). Between the tumor and the lymph node is adipose tissue containing several blood vessels. *3,* HYAL1-S #1: a thrombus (*Thr*) fills a blood vessel at the periphery of the tumor (*T*). Tumor cells (*arrows*) have infiltrated the blood vessel. *4,* HYAL1-S #2: tumor cells (*arrow*) have infiltrated a lymphatic vessel (*LV*). *5,* HYAL1-S #4: clusters of cells, mostly leukocytes, are scattered in pale-staining Matrigel (*G*). *6,* HYAL1-AS #1: the tumor (*T*) does not invade skeletal muscle (*M*) or a nerve (*N*) as connective tissue (*CT*) separates them. *B,* HYAL1 and hyaluronic acid localization. *a-c,* HYAL1 localization; *d-f,* hyaluronic acid localization. *a* and *d,* vector #1; *b* and *e,* HYAL1-S #1; *c* and *f,* HYAL1-AS #1. *C,* localization of microvessels. The areas of the highest microvessel density from each type of tumor specimen are presented; magnification, ×400. *a,* vector #1; *b,* HYAL1-S #1; *c,* HYAL1-S #2; *d,* HYAL1-AS #1. HYAL1-S #3 and #4 were not stained for hyaluronic acid, HYAL1, or microvessels as the specimen was tumor cell–free.

Discussion

The results of our study help to explain contradictory findings about the role of HYAL1 as a tumor promoter or suppressor. Whereas in some cancers hyaluronidase (i.e., HYAL1 or PH20) serves as a diagnostic or prognostic indicator, in others, hyaluronidase levels slightly decrease in high-grade tumors (6, 9–12, 18, 45–47). In bladder cancer, blocking HYAL1 expression decreases tumor growth, invasion, and angiogenesis, but in a rat colon cancer line, HYAL1 expression suppresses tumor growth and induces necrosis (29, 35). Two possibilities can explain these contradictory results: (*a*) hyaluronidases (and HYAL1 in particular) function either as tumor promoters or suppressors depending on the tumor type; (*b*) tumor promoter and suppressor functions of hyaluronidase/HYAL1 are concentration dependent.

Our data on two prostate cancer lines show that in the same tumor cell system, HYAL1 acts as a tumor suppressor and as a tumor promoter, depending on its concentration. For example, as is the case in bladder cancer (29), HYAL1-AS transfectants of prostate cancer cells grow 4-fold slower *in vitro*, are blocked in the G_2-M phase of the cell cycle, are less invasive, and generate small, less angiogenic, noninvasive tumors. HYAL1 expression in PC-3 cells has also been shown to increase their metastatic potential (30). Therefore, HYAL1 is necessary for tumor growth, invasion, and angiogenesis.

Mean hyaluronidase levels in high-grade prostate cancer tissues ($\sim$36 milliunits/mg protein) are comparable to the hyaluronidase activity (14-40 milliunits/10^6 cells) secreted by vector and moderately overproducing HYAL1 transfectants of DU145 and PC-3 ML cells (7). This suggests that the hyaluronidase concentration found in tumor tissues is in the range that is stimulatory to tumor growth, invasion, and angiogenesis.

Our data show that hyaluronidase levels of $\geq$80 to 100 milliunits/10^6 cells slow tumor cell growth *in vitro*, inhibit tumor generation by DU145 transfectants, and decrease growth of PC-3 ML tumors. Consistent with these observations, in the study that reported HYAL1 expression suppresses tumor growth in a rat colon carcinoma cell model, the transfectants expressed 220 to 360 milliunits hyaluronidase activity/10^6 cells (35). In the study involving bladder cancer cells in which we showed HYAL1 enhances tumor growth, invasion, and angiogenesis, HYAL1-S transfectants produced only 2- to 2.5-fold more hyaluronidase activity than vector transfectants (29). It is possible that in that study, high HYAL1 producing transfectants grew extremely slowly and did not form clones. Our results show that high HYAL1 producing prostate cancer cells undergo apoptosis. Furthermore, partially purified HYAL1 induces apoptosis in DU145 vector and HYAL1-S #1 and #2 clones.[5] This finding may be important in cancer treatment, as tumor cells which either do not express or moderately overexpress HYAL1 can be induced to undergo apoptosis by exposing them to HYAL1 concentration of >100 milliunits/mL.

Although the mechanism by which HYAL1 induces apoptosis in tumor cells is not fully understood, our data show that high HYAL1 expression-induced apoptosis in prostate cancer cells involves mitochondria and is possibly mediated by increased WOX1 expression and its activation. WOX1-induced apoptosis involves a mitochondrial pathway, resulting in mitochondrial permeabilization (38). Increased WOX1 expression has been shown in benign prostatic hyperplasia, prostate cancer, and metastasis (48). WOX1 may also be activated by androgens in an androgen receptor–independent manner (48). However, the functional significance of these observations is unknown.

Nearly a decade ago, it was shown that treatment with testicular hyaluronidase overcomes acquired drug resistance displayed by tumor cells growing in multicellular spheroids (49). Similarly, a clinical study conducted a few years ago showed that infusion of high doses of bovine testicular hyaluronidase (>100,000 units/kg) improves the efficacy of cytotoxic drugs (50). In these studies, it was believed that hyaluronidase played a passive role by improving drug penetration. However, such high levels of hyaluronidase may also aid in controlling tumor growth by inducing apoptosis.

Taken together, our study helps to resolve the contradiction about the role of HYAL1 as a tumor promoter and a suppressor. This study may also provide a basis for possible anti-hyaluronidase (hyaluronidase inhibition) and high-hyaluronidase treatments for controlling cancer growth and progression.

Acknowledgments

Received 3/28/2005; revised 6/9/2005; accepted 6/16/2005.

Grant support: Department of Defense grant DAMD 170210005 (V.B. Lokeshwar) and NIH/National Cancer Institute grants RO1 072821-06 (V.B. Lokeshwar) and 2RO1-CA061038 (B.L. Lokeshwar).

The costs of publication of this article were defrayed in part by the payment of page charges. This article must therefore be hereby marked *advertisement* in accordance with 18 U.S.C. Section 1734 solely to indicate this fact.

We thank Dr. Awtar Krishan Ganju, Department of Pathology, for his advice on flow cytometry. We thank Dr. Charles Clifford, Director of Pathology, Charles River Laboratories (Wilmington, MA), for his help in histology. Dr. Tadahiro Isoyama was supported by Tottori University Hospital, Yonago, Japan. We gratefully acknowledge the editorial assistance of Marie G. Selzer, Department of Urology, University of Miami (Miami, FL).

[5] Unpublished results.

References

1. Toole BP. Hyaluronan: from extracellular glue to pericellular cue. Nat Rev Cancer 2004;4:528–39.
2. Tammi MI, Day AJ, Turley EA. Hyaluronan and homeostasis: a balancing act. Biol Chem 2002;277:4581–4.
3. Turley EA, Noble PW, Bourguignon LY. Signaling properties of hyaluronan receptors. J Biol Chem 2002;277:4589–92.
4. Setälä LP, Tammi MI, Tammi RH, et al. Hyaluronan expression in gastric cancer cells is associated with local and nodal spread and reduced survival rate. Br J Cancer 1999;79:1133–8.
5. Auvinen P, Tammi R, Parkkinen J, et al. Hyaluronan in peritumoral stroma and malignant cells associates with breast cancer spreading and predicts survival. Am J Pathol 2000;156:529–36.
6. Hautmann SH, Lokeshwar VB, Schroeder GL, et al. Elevated tissue expression of hyaluronic acid and hyaluronidase validates the HA-HAase urine test for bladder cancer. J Urol 2001;165:2068–74.
7. Lokeshwar VB, Rubinowicz D, Schroeder GL, et al. Stromal and epithelial expression of tumor markers hyaluronic acid and HYAL1 hyaluronidase in prostate cancer. J Biol Chem 2001;276:11922–32.
8. Lipponen P, Aaltomaa S, Tammi R, Tammi M, Ågren U, Kosma VM. High stromal hyaluronan level is associated with poor differentiation and metastasis in prostate cancer. Eur J Cancer 2001;37:849–56.
9. Lokeshwar VB, Obek C, Soloway MS, Block NL. Tumor-associated hyaluronic acid: a new sensitive and specific urine marker for bladder cancer. Cancer Res 1997;57:773–7. Erratum in: Cancer Res 1998;58:3191.
10. Lokeshwar VB, Obek C, Pham HT, et al. Urinary hyaluronic acid and hyaluronidase: markers for bladder cancer detection and evaluation of grade. J Urol 2000;163:348–56.
11. Posey JT, Soloway MS, Ekici S, et al. Evaluation of the prognostic potential of hyaluronic acid and hyaluronidase (HYAL1) for prostate cancer. Cancer Res 2003;63:2638–44.

12. Ekici S, Cerwinka WH, Duncan R, et al. Comparison of the prognostic potential of hyaluronic acid, hyaluronidase (HYAL-1), CD44v6 and microvessel density for prostate cancer. Int J Cancer 2004;112:121–9.

13. Hayen W, Goebeler M, Kumar S, Riessen R, Nehls V. Hyaluronan stimulates tumor cell migration by modulating the fibrin fiber architecture. J Cell Sci 1999;112:2241–51.

14. Hobarth K, Maier U, Marberger M. Topical chemoprophylaxis of superficial bladder cancer with mitomycin C and adjuvant hyaluronidase. Eur Urol 1992;21:206–10.

15. Itano N, Atsumi F, Sawai T, et al. Abnormal accumulation of hyaluronan matrix diminishes contact inhibition of cell growth and promotes cell migration. Proc Natl Acad Sci 2002;99:3609–14.

16. Lees VC, Fan TP, West DC. Angiogenesis in a delayed revascularization model is accelerated by angiogenic oligosaccharides of hyaluronan. Lab Invest 1995;73:259–66.

17. West DC, Hampson IN, Arnold F, Kumar S. Angiogenesis induced by degradation products of hyaluronic acid. Science 1985;228:1324–6.

18. Franzmann EJ, Schroeder GL, Goodwin WJ, Weed DT, Fisher P, Lokeshwar VB. Expression of tumor markers hyaluronic acid and hyaluronidase (HYAL1) in head and neck tumors. Int J Cancer 2003;106:438–45.

19. Girish KS, Shashidharamurthy R, Nagaraju S, Gowda TV, Kemparaju K. Isolation and characterization of hyaluronidase a "spreading factor" from Indian cobra (*Naja naja*) venom. Biochemie 2004;86:193–202.

20. Kuhn-Nentwig L, Schaller J, Nentwig W. Biochemistry, toxicology and ecology of the venom of the spider *Cupiennius salei* (*Ctenidae*). Toxicon 2004;43:543–53.

21. Csoka AB, Frost GI, Stern R. The six hyaluronidase-like genes in the human and mouse genomes. Matrix Biol 2001;20:499–508.

22. Cherr GN, Yudin AI, Overstreet JW. The dual functions of GPI-anchored PH-20: hyaluronidase and intracellular signaling. Matrix Biol 2001;20:515–25.

23. Csoka AB, Frost GI, Wong T, Stern R. Purification and microsequencing of hyaluronidase isozymes from human urine. FEBS Lett 1997;417:307–10.

24. Frost GI, Csoka AB, Wong T, Stern R. Purification, cloning, and expression of human plasma hyaluronidase. Biochem Biophys Res Commun 1997;236:10–5.

25. Triggs-Raine B, Salo TJ, Zhang H, Wicklow BA, Natowicz MR. Mutations in HYAL1, a member of a tandemly distributed multigene family encoding disparate hyaluronidase activities, cause a newly described lysosomal disorder, mucopolysaccharidosis IX. Proc Natl Acad Sci U S A 1999;96:6296–300.

26. Lokeshwar VB, Young MJ, Goudarzi G, et al. Identification of bladder tumor-derived hyaluronidase: its similarity to HYAL1. Cancer Res 1999;59:4464–70.

27. Victor R, Chauzy C, Girard N, et al. Human breast-cancer metastasis formation in a nude-mouse model: studies of hyaluronidase, hyaluronan and hyaluronan-binding sites in metastatic cells. Int J Cancer 1999;82:77–83.

28. Madan AK, Yu K, Dhurandhar N, Cullinane C, Pang Y, Beech DJ. Association of hyaluronidase and breast adenocarcinoma invasiveness. Oncol Rep 1999;6:607–9.

29. Lokeshwar VB, Cerwinka WH, Lokeshwar BL. HYAL1 hyaluronidase: a molecular determinant of bladder cancer growth and progression. Cancer Res 2005;65:2243–50.

30. Patel S, Turner PR, Stubberfield C, et al. Hyaluronidase gene profiling and role of hyal-1 overexpression in an orthotopic model of prostate cancer. Int J Cancer 2002;97:416–24. Erratum in: Int J Cancer 2002;98:957.

31. Junker N, Latini S, Petersen LN, Kristjansen PE. Expression and regulation patterns of hyaluronidases in small cell lung cancer and glioma lines. Oncol Rep 2003;10:609–16.

32. Csoka AB, Frost GI, Heng HH, Scherer SW, Mohapatra G, Stern R. The hyaluronidase gene HYAL1 maps to chromosome 3p21.2-p21.3 in human and 9F1-F2 in mouse, a conserved candidate tumor suppressor locus. Genomics 1998;48:63–70.

33. Ji L, Nishizaki M, Gao B, et al. Expression of several genes in the human chromosome 3p21.3 homozygous deletion region by an adenovirus vector results in tumor suppressor activities *in vitro* and *in vivo*. Cancer Res 2002;62:2715–20.

34. Bertrand P, Courel MN, Maingonnat C, Jardin F, Tilly H, Bastard C. Expression of HYAL2 mRNA, hyaluronan and hyaluronidase in B-cell non-Hodgkin lymphoma: relationship with tumor aggressiveness. Int J Cancer 2005;113:207–12.

35. Jacobson A, Rahmanian M, Rubin K, Heldin P. Expression of hyaluronan synthase 2 or hyaluronidase 1 differentially affect the growth rate of transplantable colon carcinoma cell tumors. Int J Cancer 2002;102:212–9.

36. Shuster S, Frost GI, Csoka AB, Formby B, Stern R. Hyaluronidase reduces human breast cancer xenografts in SCID mice. Int J Cancer 2002;102:192–7.

37. Chang NS. Hyaluronidase activation of c-Jun N-terminal kinase is necessary for protection of L929 fibrosarcoma cells from staurosporine-mediated cell death. Biochem Biophys Res Commun 2001;283:278–86.

38. Chang NS, Doherty J, Ensign A, et al. Molecular mechanisms underlying WOX1 activation during apoptotic and stress responses. Biochem Pharmacol 2003;66:1347–54.

39. Chang NS, Pratt N, Heath J, et al. Hyaluronidase induction of a WW domain-containing oxidoreductase that enhances tumor necrosis factor cytotoxicity. J Biol Chem 2001;276:3361–70.

40. Chang NS. Transforming growth factor-β1 blocks the enhancement of tumor necrosis factor cytotoxicity by hyaluronidase Hyal-2 in L929 fibroblasts. BMC Cell Biol 2002;3:8.

41. Pham HT, Block NL, Lokeshwar VB. Tumor-derived hyaluronidase: a diagnostic urine marker for high-grade bladder cancer. Cancer Res 1997;57:778–83. Erratum in: Cancer Res 1997;57:1622.

42. Lokeshwar BL, Selzer MG, Zhu BQ, Block NL, Golub LM. Inhibition of cell proliferation, invasion, tumor growth and metastasis by an oral non-antimicrobial tetracycline analog (COL-3) in a metastatic prostate cancer model. Int J Cancer 2002;98:297–309.

43. Zoltan-Jones A, Huang L, Ghatak S, Toole BP. Elevated hyaluronan production induces mesenchymal and transformed properties in epithelial cells. J Biol Chem 2003;278:45801–10.

44. Dandekar DS, Lokeshwar BL. Inhibition of cyclo-oxygenase (COX)-2 expression by Tet-inducible COX-2 antisense cDNA in hormone-refractory prostate cancer significantly slows tumor growth and improves efficacy of chemotherapeutic drugs. Clin Cancer Res 2004;10:8037–47.

45. Beech DJ, Madan AK, Deng N. Expression of PH-20 in normal and neoplastic breast tissue. J Surg Res 2002;103:203–7.

46. Tuhkanen H, Anttila M, Kosma VM, et al. Genetic alterations in the peritumoral stromal cells of malignant and borderline epithelial ovarian tumors as indicated by allelic imbalance on chromosome 3p. Int J Cancer 2004;109:247–52.

47. Hiltunen EL, Anttila M, Kultti A, et al. Elevated hyaluronan concentration without hyaluronidase activation in malignant epithelial ovarian tumors. Cancer Res 2002;62:6410–3.

48. Chang NS, Schultz L, Hsu LJ, Lewis J, Su M, Sze CI. 17β-Estradiol up-regulates and activates WOX1/WWOXv1 and WOX2/WWOXv2 *in vitro*: potential role in cancerous progression of breast and prostate to a premetastatic state *in vivo*. Oncogene 2005;24:714–23.

49. Croix BS, Rak JW, Kapitain S, Sheehan C, Graham CH, Kerbel RS. Reversal by hyaluronidase of adhesion-dependent multicellular drug resistance in mammary carcinoma cells. J Natl Cancer Inst 1996;88:1285–96.

50. Klocker J, Sabitzer H, Raunik W, Wieser S, Schumer J. Hyaluronidase as additive to induction chemotherapy in advanced squamous cell carcinoma of the head and neck. Cancer Lett 1998;131:113–5.